Widening the prospects for gallium oxide power electronics

Mike Cooke reports on research on gallium oxide as a wider-bandgap semiconductor than gallium nitride and silicon carbide.

Scientists and engineers are on the constant look-out for materials that may help create effective new technologies. There is increasing demand for 'smart' compact power electronics systems, which need to be able to handle high electric fields. Materials with wider bandgaps should in principle support larger electric fields. The drawback is that wide bandgaps mean that the materials are more insulating and less semiconducting. In wide-bandgap materials that allow conduction with suitable doping there is usually a trade-off between high breakdown voltages and low on-resistance.

A recent power electronics

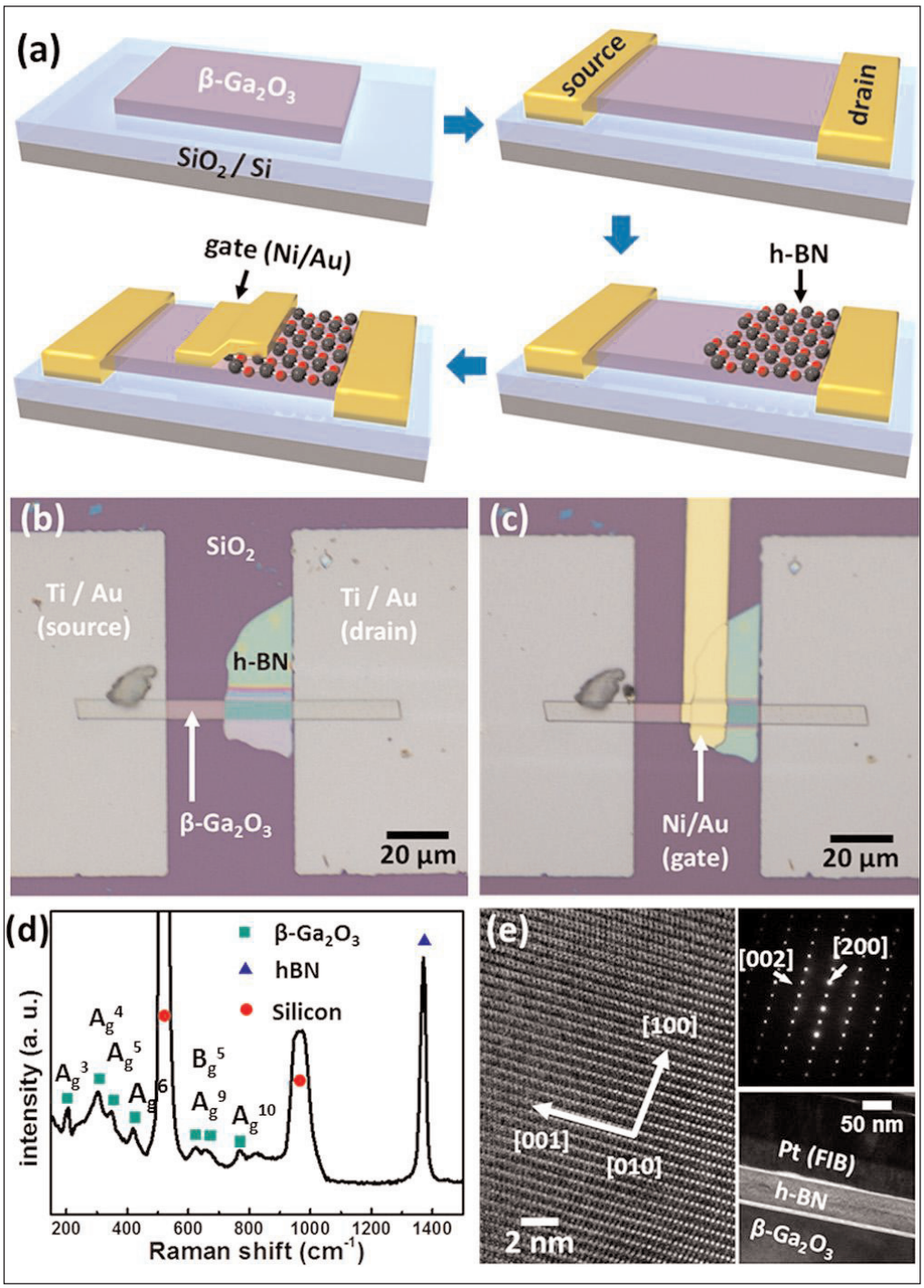

Figure 1. (a) Schematic fabrication process for nano-layer β-Ga_2O_3 MESFET with h-BN field plate. Optical microscopy images (b) before and (c) after the deposition of top-gate electrode (Ni/Au). (d) Raman spectra of fabricated h-BN/β-Ga_2O_3 structure. (e) Cross-sectional high-resolution transmission electron microscope TEM image of β-Ga_2O_3. Insets show selected-area diffraction patterns of β-Ga_2O_3 flakes (top), and a cross section of stacked layers of platinum (Pt) from focused ion beam (FIB) sample preparation and h-BN/β-Ga_2O_3 heterostructure (bottom).

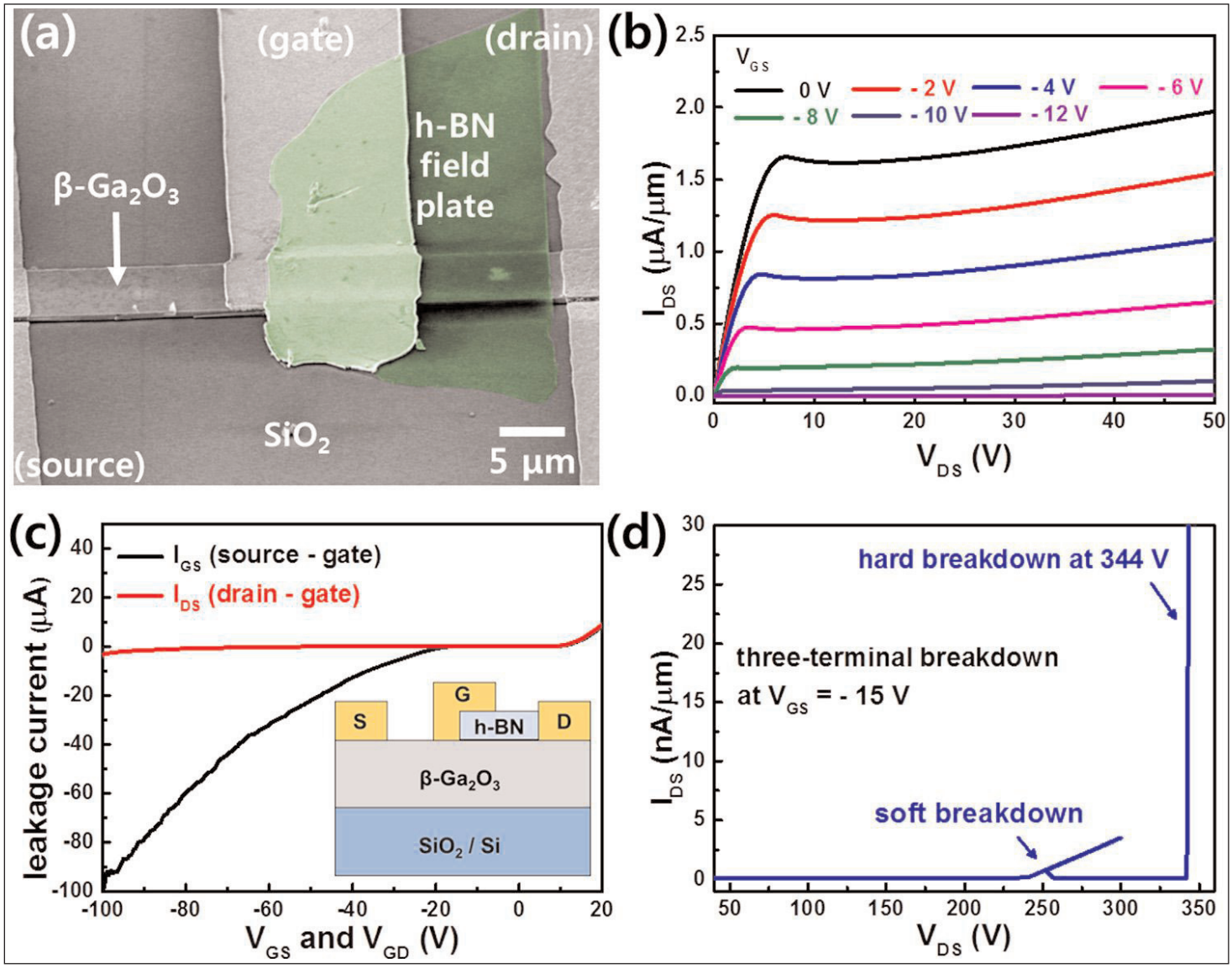

Figure 2. (a) False-color scanning electron microscope image of exfoliated quasi-two-dimensional β-Ga_2O_3 field-plate MESFET. (b) DC output characteristics of MESFET drain current (I_{DS}) versus bias (V_{DS}) for various gate potentials (V_{GS}). (c) Two-terminal gate leakage current in source–gate and drain–gate regions (inset: schematic of fabricated MESFET). (d) Off-state three-terminal breakdown curve showing soft and hard breakdown voltages.

contender is gallium oxide, generally with the more stable beta crystal structure (β-Ga_2O_3). Devices based on β-Ga_2O_3 are being developed in the hope of power electronics applications, based on an ultra-wide 4.5–4.9eV direct bandgap and good thermal stability. These bandgap energies are larger than for competitors such as gallium nitride (3.4eV), silicon carbide (~3eV) or silicon (1.12eV). Theory also suggests that β-Ga_2O_3 has potential for high saturation velocity (~2x10^7cm/s) and breakdown field (8MV/cm).

The Baliga and Johnson figures of merit for β-Ga_2O_3 are 3214.1 and 2844.4, respectively, which correspondingly compare with gallium nitride's 846.0 and 1089.0, and with silicon carbide's 317.1 and 277.8. These figures focus on the suitability of the material for high-frequency power electronics and low on-resistance.

Another development is larger-diameter commercial β-Ga_2O_3 substrates beyond the 2" of gallium nitride.

These features could be brought to bear on power amplifier applications in the RF and millimeter-wave regimes, especially at high frequencies and high power densities that are enabled by high thermal conductivity.

Devices based on β-Ga_2O_3 are n-type 'unipolar', depending on negative charge carriers, due to the lack of a suitable p-type dopant. The donor dopants for n-type conductivity include group IV elements such as silicon, germanium and tin. Also, background unintentional n-type 'doping' can occur according to different growth conditions, which can lead to oxygen vacancies or hydrogen inclusion. The restriction to unipolar conductivity limits device architectures.

Developments are at an early stage, and generally devices don't reach the performance of more established technologies. Here, we report on recent research.

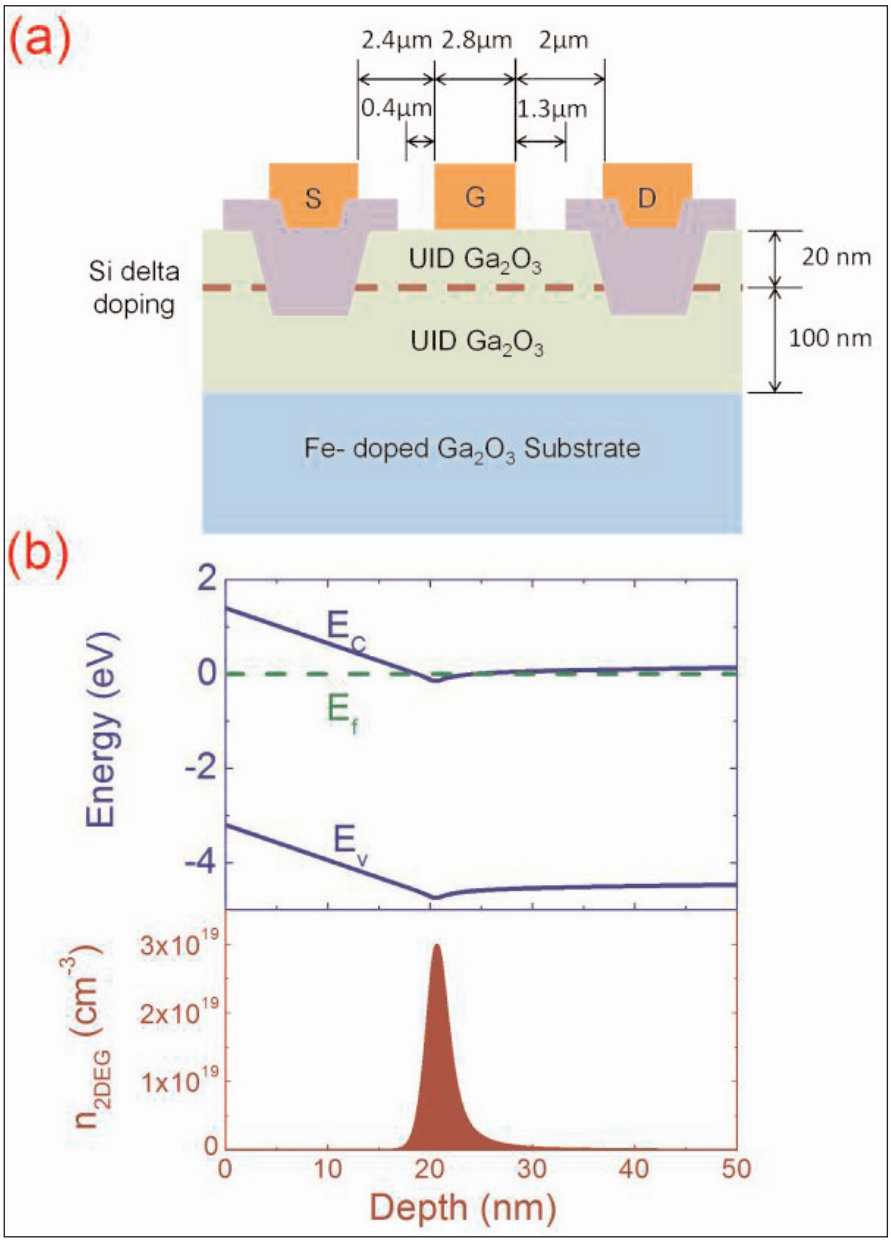

Figure 3. (a) Device schematic and (b) equilibrium energy-band diagram and 2DEG charge profile of delta doped MESFET.

Field-effect transistors

Korea University and Korea Electrotechnology Research Institute (KERI) have used hexagonal boron nitride (h-BN) as part of a field-plate structure for β-Ga_2O_3 metal-semiconductor field-effect transistors (MESFETs) [Jinho Bae et al, Appl. Phys. Lett., vol112, p122102, 2018]. The off-state breakdown reached 344V.

The researchers used single-crystal β-Ga_2O_3 substrate from Tamura Corp for the transistor (Figure 1). The material was mechanically exfoliated into quasi-two-dimensional flakes 200–400nm thick using adhesive tape. The flakes were transferred onto a 300nm silicon dioxide layer on a 500μm-thick silicon substrate.

Ohmic source–drain electrodes consisted of annealed titanium/gold. The ~70nm-thick h-BN field-plate insulation material was mechanically exfoliated from bulk powder supplied by Momentive Corp. The transfer to the transistor was assisted using transparent gel-film from Gel-pak to allow for precise positioning. The top gate electrode was nickel/gold.

In addition to having a high dielectric breakdown field of 8–12MV/cm, the h-BN has a high thermal conductivity of 1700–2000W/m-K. The h-BN crystal structure has van der Waals forces linking 'two-dimensional' hexagonal layers, allowing thin flakes to be produced by mechanical exfoliation. While β-Ga_2O_3 is not structured in this way, it does have bond anisotropy that favors cleavage along the (100) face of the crystal lattice. The researchers suggest that thinner β-Ga_2O_3 could be obtained with reactive-ion and/or inductively coupled plasma etch.

A gate potential of –12V gave complete pinch-off of the n-channel device (Figure 2). The threshold voltage was at –7.3V. Unlike many common 2D materials such as graphene and transition-metal dichalcogenides, these devices had a knee in the current performance with respect to drain voltage, giving a saturation region. The sub-threshold swing was relatively low, at 84.6mV/decade, indicating sharp switching behavior. Previously reported β-Ga_2O_3 transistors have had swings of more than 100mV/decade.

The soft breakdown in pinch-off (gate at –15V) occurred at 250V drain. Complete failure came at 344V. Devices without the field-plate structure broke down at 113V. The researchers suggest that more complex field-plate arrangements could improve the breakdown performance.

Without field plates, the researchers simulated a peak electric field for 200V drain bias of 7.3MV/cm, close to the ~8MV/cm critical field for β-Ga_2O_3. The simulations used to give the estimate suggest the breakdown occurs near the gate edge. With a field plate, the peak field at 200V was reduced to 4.5MV/cm.

The long-term chemical stability of the device was also investigated, since 2D structures are often vulnerable to degradation from the atmosphere. The researchers stored the device in ambient air for a month. "Device properties including on/off current ratio, saturation current, transconductance, subthreshold swing, and threshold voltage were maintained," they report.

Meanwhile, the USA's Ohio State University, University of Utah and the Indian Institute of Technology in Bombay have used oxygen-plasma-assisted

molecular beam epitaxy (MBE) at 700ºC on a semi-insulating iron-doped (010) β-Ga_2O_3 substrate to produce MESFETs [Zhanbo Xia et al, IEEE Electron Device Letters, vol39, p568, 2018] (Figure 3). The substrates were mounted on silicon with indium bonding during the MBE.

A 0.2nm silicon delta-doped region was used to create a two-dimensional electron gas (2DEG) for the transistor channel. The source and drain regions were re-grown heavily n-type doped β-Ga_2O_3 in 40nm-deep trenches. The ohmic contacts for the source and drain were annealed titanium/gold/nickel. After mesa isolation, the nickel/gold/nickel Schottky gate metal was applied.

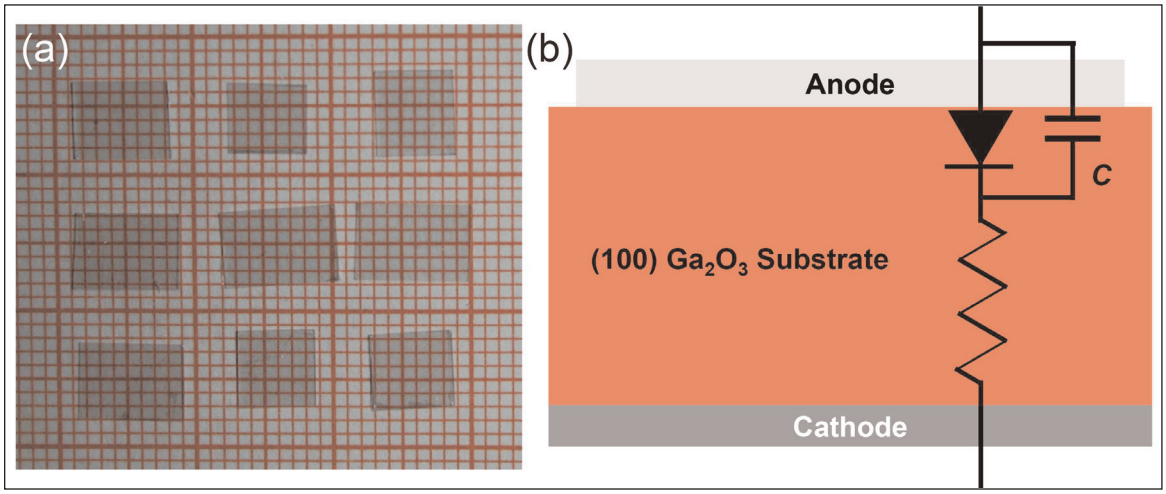

Figure 4. (a) (100) β-Ga_2O_3 substrates used for Schottky barrier diode fabrication. (b) Schematic structure and equivalent circuit of Pt/(100)β-Ga_2O_3 Schottky barrier diode.

Devices based on β-Ga_2O_3 are n-type 'unipolar', depending on negative charge carriers, due to the lack of a suitable p-type dopant. The donor dopants for n-type conductivity include group IV elements such as silicon, germanium and tin. The restriction to unipolar conductivity limits device architectures

A device with 2.8μm gate length achieved a normalized maximum drain current of 140mA/mm at +2V gate potential and 10V drain bias, across a 100μm width. The gate–source and gate–drain separations were 0.4μm and 1.3μm, respectively. A peak transconductance of 34mS/mm was found with +0.5V on the gate. The threshold voltage was estimated at −3.4V — i.e. the device is normally-on.

The on/off current ratio was of the order 10^5. With the gate at −5V, the three-terminal breakdown occurred at 170V drain bias for a 0.1mA/mm leakage current. The peak electron mobility was estimated to be 95cm^2/V-s. The researchers comment: "Further theoretical analysis is required to understand the detailed scattering mechanisms that limit 2DEG mobility."

Schottky barrier diodes

Researchers based in China have reported on β-Ga_2O_3 Schottky barrier diodes with AC rectification assessed up to 1MHz [Qiming He et al, IEEE Electron Device Letters, vol39, p556, 2018]. The team from Xiangtan University, Jiangsu National Synergetic Innovation Center for Advanced Materials (SICAM), Shandong University and Sun Yat-sen University found that the devices demonstrated a short reverse recovery time of 20ns.

Edge-defined film-fed growth (EFG) gave blocks of (100)-oriented β-Ga_2O_3 smaller than 10mm x 10mm and 480nm thick. EFG creates ribbons of crystalline material pulled from a melt through a 'die'. Optimization of the growth process in terms of temperature control and seeding improved the crystal structure. Tin dioxide (SnO_2) powder was used for n-type doping, giving a carrier density of 2x10^{17}/cm^3 determined from Hall-effect and capacitance–voltage measurements. Mechanical exfoliation reduced surface roughness to 0.1nm root-mean-square.

The Schottky barrier diodes used platinum for the 150μm-diameter Schottky circular anode contact (Figure 4). The ohmic cathode metal was titanium, which was optimized with a 400ºC oxygen plasma pre-treatment. The contact stacks (Pt/Ti/Au and Ti/Au) were deposited by magnetron sputtering.

The forward current density was 421A/cm^2 at 2V bias, a seven-fold improvement on the group's previous work. The on-resistance was reduced from the previous 12.5mΩ-cm^2 to 2.9mΩ-cm^2. Under reverse bias of −200V, the current was 2.3x10^{-4}A/cm^2. The leakage was somewhat higher than the previous work. The team suggests that this can be reduced with epitaxial device layers, field plates and rings, and/or trench structures. The test equipment was unable to take the device to breakdown.

Frequency-dependent capacitance-voltage studies gave a built-in potential of 0.63V. This was lower than the 1.07V normally given — the team suggests that this is due to a higher-than-usual carrier density in the β-Ga_2O_3. The recovery time from 4V forward to −10V reverse bias was 20ns. With a 20V peak-to-peak AC signal, the device rectified the sine input into half-sine output at frequencies up to 1MHz. At 1MHz, there was a slight negative current attributed to junction capaci-

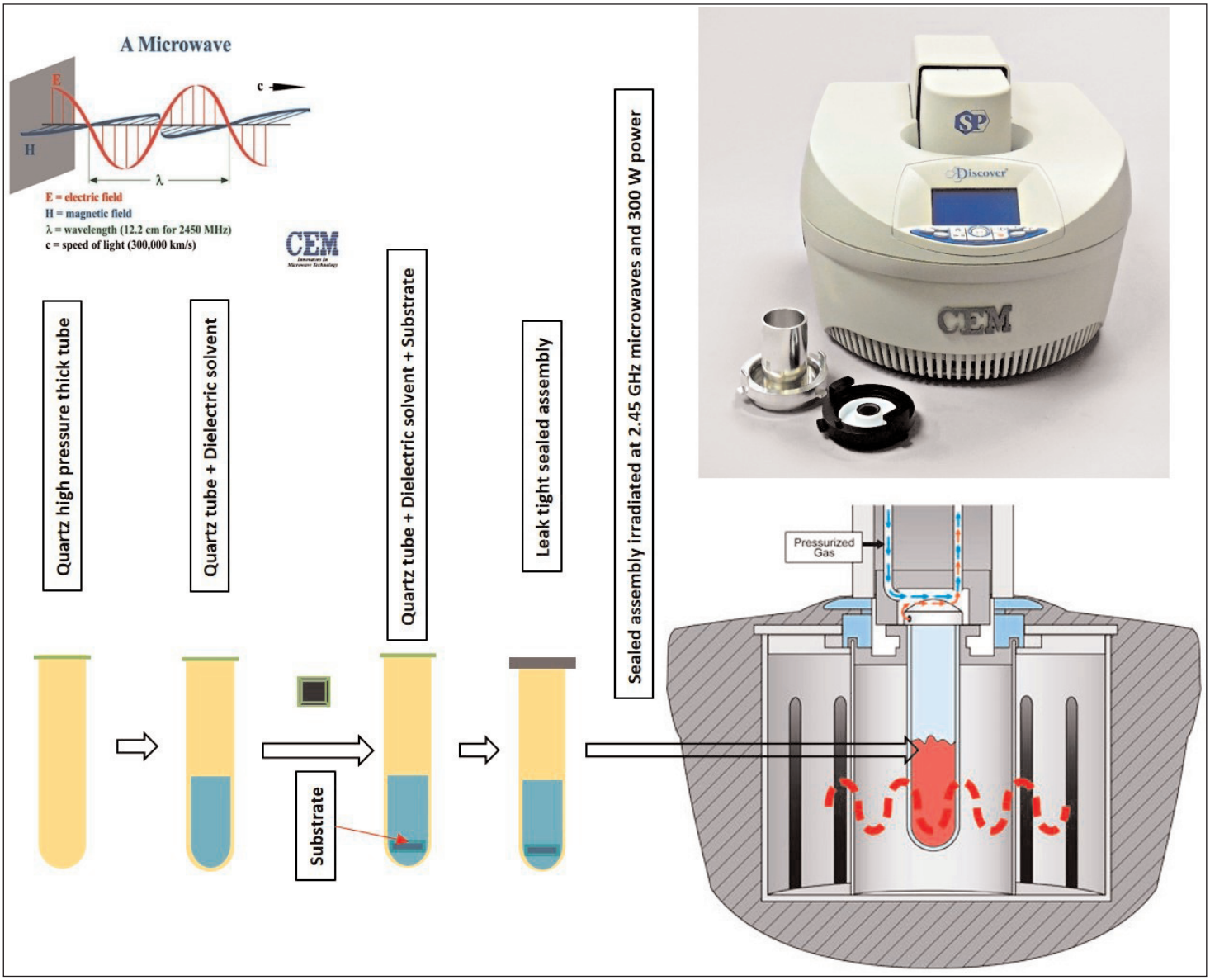

Figure 5. Schematic representation of microwave-irradiation-assisted film deposition process.

tance. The researchers say this capacitance could be reduced by reducing the doping in an epitaxial layer or by using ultra-thin wafers.

Researchers based in USA and India have produced bevel-field-plated Schottky barrier diodes [Chandan Joishi et al, Appl. Phys. Express, vol11, p031101, p2018]. Breakdown occurred at −190V and the device was able to withstand 1A/cm^2 before catastrophic damage. Repeatable breakdown for 0.2A/cm^2 compliance was −129V. The estimated peak breakdown field (F_{BR}) was 4.2MV/cm, which compares with the 8MV/cm theoretical critical field for β-Ga_2O_3.

The team from Ohio State University, the Indian Institute of Technology Bombay, and the USA's Case Western Reserve University and University of Utah adds: "The extracted F_{BR} is higher than the theoretical F_{BR} values for 4H-SiC (2.2MV/cm) and GaN (3.3MV/cm)." This research grouping partly overlaps that for the MESFET of Zhanbo Xia et al above.

The edge field was estimated at 5.9MV/cm. The extrinsic on-resistance was 3.9mΩ-cm^2 — the intrinsic value was 0.023mΩ-cm^2. The difference between the two values is attributed to the resistance of the substrate.

The researchers grew 2mm of β-Ga_2O_3 on a commercial tin-doped (Sn) (010) β-Ga_2O_3 substrate by low-pressure chemical vapor deposition (LPCVD) using gallium from high-purity pellets and oxygen in argon carrier gas. Silicon n-type doping was achieved with silicon tetrachloride. Atomic force microscopy on the epitaxial surface gave a roughness value of 4.86nm root-mean-square.

Platinum/nickel/gold (Pt/Ni/Au) was used as a 50mm x 1mm beveled stripe anode. The electrode had rounded corners to avoid the formation of spherical junctions under high bias. The titanium/gold/nickel (Ti/Au/Ni) cathode was deposited on the substrate side of the device. The bevel anode was covered with plasma-enhanced CVD silicon dioxide surface passivation and a field plate formed from titanium that extended out 4μm (L_{FP}). The distance from the start of the bevel and the anode electrode (L_{AB}) was 0.25μm.

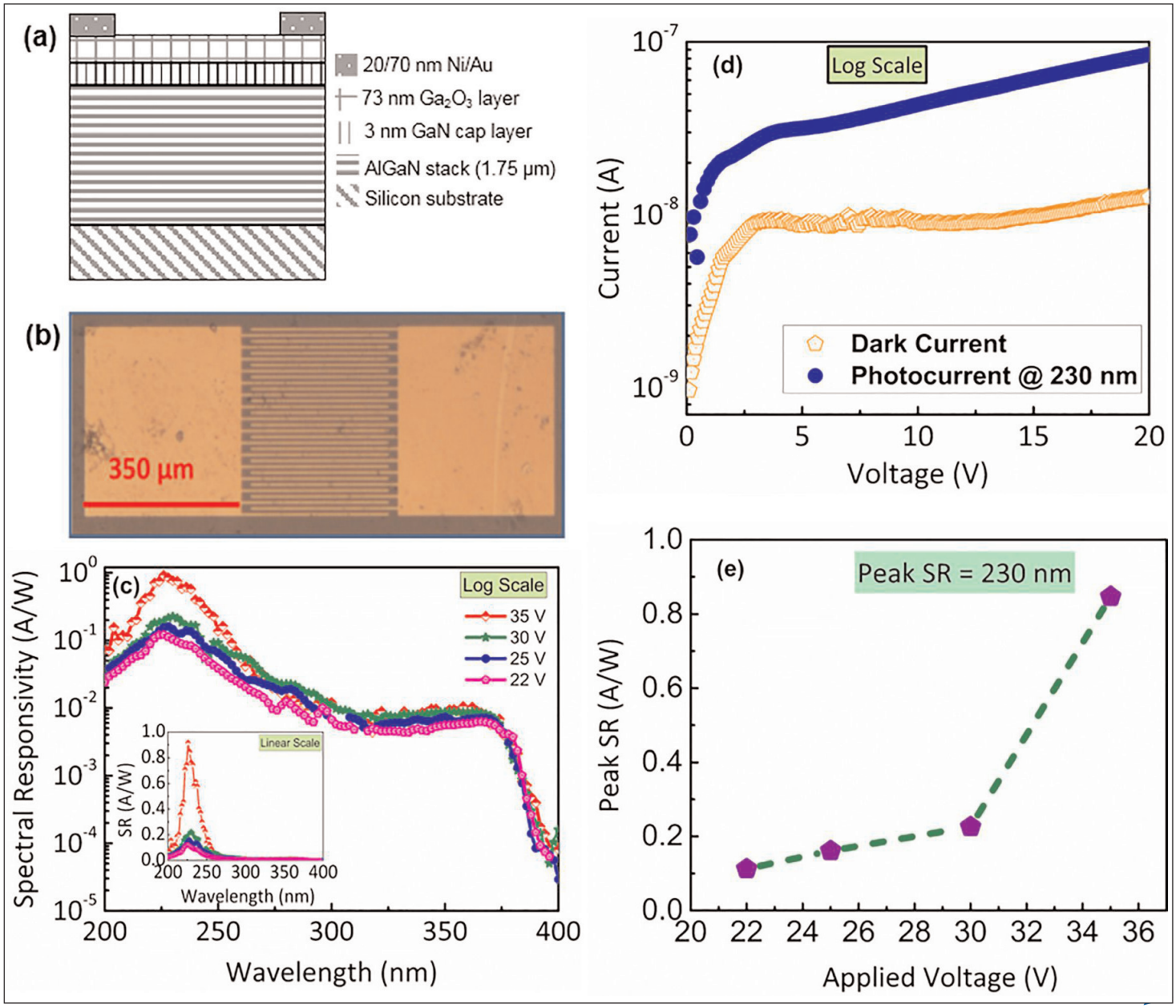

Figure 6. (a) Schematic of AlGaN/GaN HEMT stack (side-view). (b) Optical micrograph of fabricated MSM device (top-view). (c) Variation of spectral response (SR) with wavelength on log scale as function of bias. Inset: variation of SR with wavelength as function of bias on linear scale. (d) Variation of dark and photocurrent with applied bias. Photocurrent measured under 230nm illumination. (e) Variation of peak responsivity (SR at 230nm) with applied bias (measured at optical chopping frequency of 30Hz).

III–nitride on silicon substrate

The Indian Institute of Science has also been developing microwave polycrystal deposition of β-Ga_2O_3 on gallium nitride (GaN) on silicon with a view to deep ultraviolet (UV) optoelectronics [Piyush Jaiswal et al, Appl. Phys. Lett., vol112, p021105, 2018]. The team also demonstrated a visible-blind 230nm-wavelength deep UV photodetector based on the wide bandgap of β-Ga_2O_3 material.

The absorption edge for β-Ga_2O_3 is in the wavelength range 240–250nm. Meanwhile, GaN has been developed for visible and near-UV light emission, along with, more recently, high-voltage and high-current-density electronics and for operation at high switching speeds. Bringing these technologies together, the researchers target heterostructures and devices that would exploit bandgap engineering opportunities.

The Ga_2O_3 was deposited on III–nitrides by microwave irradiation of a reactant solution containing Ga(III)acetyl-acetonate, a β-ketonate complex (see Figure 5). The solvent was a mix of ethanol and 1-decanol. The substrate was a GaN stack with aluminium gallium nitride (AlGaN) layers typically designed for high-electron-mobility transistors (HEMTs).

"Epitaxially grown GaN layers were used as substrates, because of the close lattice match between h-GaN and β-Ga_2O_3 along the (100) direction," the team comments. Temperatures during the deposition did not exceed

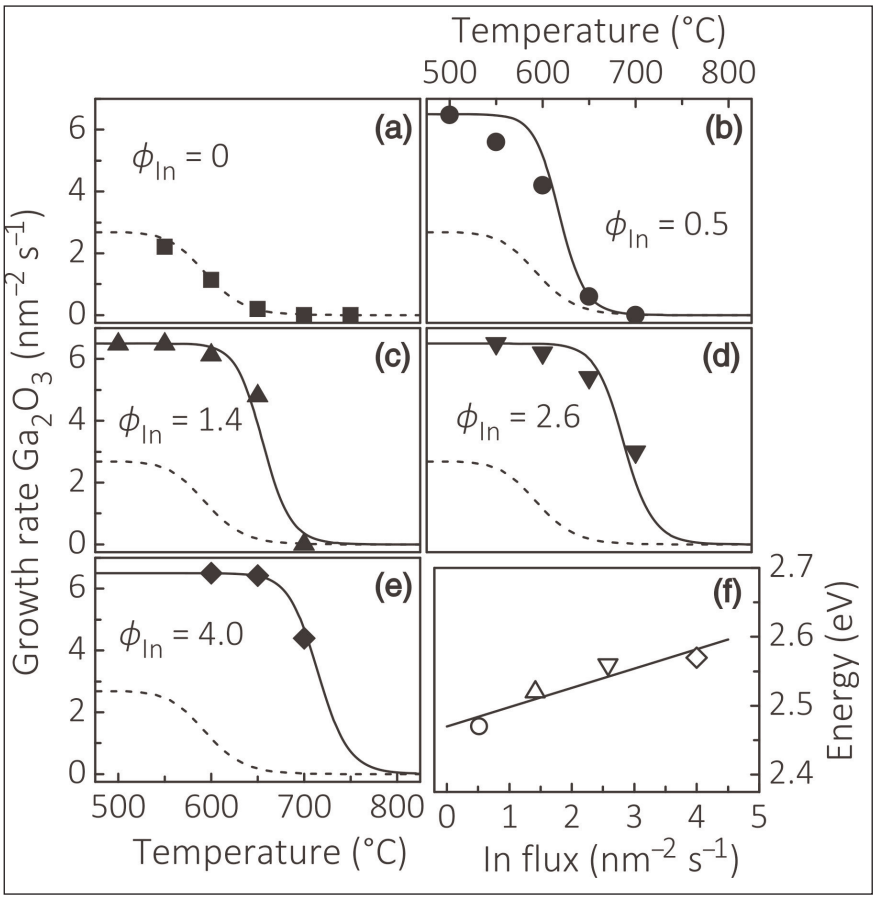

Figure 7. (a)–(e) Temperature dependence of Ga_2O_3 growth rate with varying indium flux (ϕ_{In} in units of $nm^{-2}s^{-1}$). The gallium flux was 6.5/nm^2-s. (f) Activation energy of In desorption as function of ϕ_{In}.

200ºC. The duration was less than an hour, including thermal ramp up and down.

X-ray photoelectron spectroscopy (XPS) of the β-Ga_2O_3 did not find any nitrogen, suggesting uniform coverage of the III–nitride layers. Further findings were some carbon from the organic solvents and an oxygen deficiency leading to vacancies and an expectation of n-type conductivity.

X-ray diffraction studies suggested a nano-crystalline Ga_2O_3 structure with an estimated thickness of 70–80nm. The average crystallite size was 3.3nm and the material was in the gamma(γ)-phase. Rapid thermal annealing at 950ºC for 10 minutes converted the phase to β with 22.4nm crystallites.

The researchers comment: "The counter-intuitive formation of γ-Ga_2O_3 at sub-200ºC is attributable to locally elevated temperatures in the irradiated solution and to the nucleation kinetics of γ-Ga_2O_3 formation because γ-Ga_2O_3 has a spinel structure associated with many vacancies, and crystals containing vacant sites are stabilized at low crystallization temperatures."

The x-ray results were backed up with scanning electron microscopy and atomic force microscopy.

Nickel/gold Schottky contacts were deposited on the β-Ga_2O_3 layer to create a metal-semiconductor–metal photodetector (PD — see Figure 6). The electrodes consisted of 16 interdigitated fingers. The width of the fingers was 5μm and the spacing 6μm. The active area is given as 250μm x 300μm.

Peak spectral responsivity occurred at 236nm deep UV — 0.1A/W at 22V bias and 0.8A/W at 35V. Compared with the response at 400nm visible wavelengths, the rejection ratio was more than 10^3 at 22V bias. The kink downward in the response at 365nm near-UV is attributed to absorption and conduction in the narrower ~3.4eV-bandgap GaN layer beneath the β-Ga_2O_3. The dark current at 20V was ~12nA, compared with ~82nA under 230nm illumination.

The researchers suggest that the increase in peak response at 35V was due to internal gain. The team explains: "This gain comes from either an oxygen-deficient film, leading to trapping of holes in bulk, or interface states at the metal-semiconductor (M–S) Schottky junction enabling hole trapping at the M–S junction itself. As the M–S junction has to maintain charge neutrality, more electrons have to flow from the metal side, subsequently lowering the Schottky barrier, thereby leading to gain in the photodetector."

Plasma molecular beam epitaxy

Germany's Paul-Drude-Institut für Festkörperelektronik has developed epitaxy techniques for gallium oxide growth that could lead to sesquioxide heterostructures where the metal involved is aluminium (Al_2O_3), gallium (Ga_2O_3) or indium (In_2O_3) [Patrick Vogt et al, Phys. Rev. Lett., vol119, p196001, 2017]. In particular, the team found that the presence of indium during plasma-assisted molecular beam epitaxy (PAMBE) increased the growth rate of Ga_2O_3, even when there is no growth without indium.

The researchers hope that their work will be a path for bandgap engineering and heterostructural growth of transparent semiconducting oxides. They see analogies with the III–V world, where heterostructures of semiconductor alloys have created a vast range of optoelectronic and telecom devices. For the sesquioxides, the team suggests applications in deep-ultraviolet detection, transparent transistors, and high-power electronics.

One problem is that the sesquioxides tend to crystallize in incompatible structures: corundum (rhombohedral, $R\bar{3}c$) for α-Al_2O_3, gallia (monoclinic, C2/m) for β-Ga_2O_3, and bixbyite (body centered cubic, $Ia\bar{3}$) for In_2O_3. Also, the complexity of the oxide reactions leading to sesquioxides restricts growth to lower temperatures, reducing crystal quality.

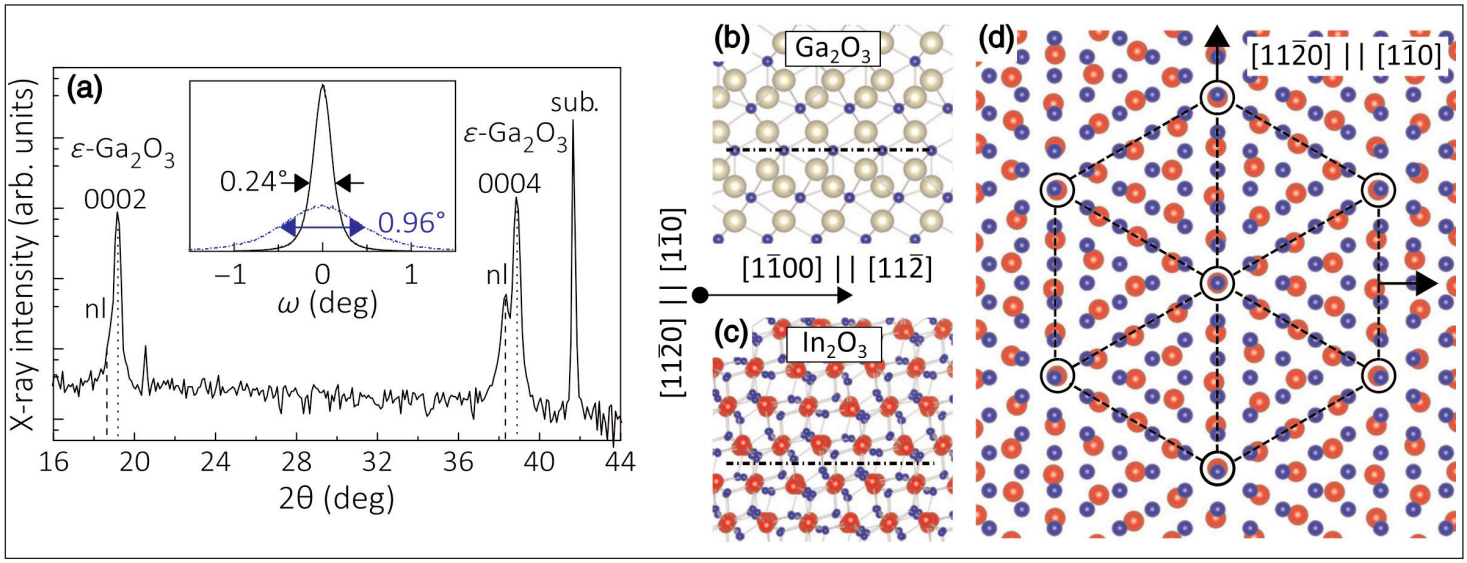

Figure 8. (a) Longitudinal x-ray diffraction scan of In_2O_3-catalyzed Ga_2O_3 700ºC film with 5.4/nm²-s indium flux. Reflections labeled 'sub.' and 'nl' stem from substrate and nucleation layer, respectively. Inset: transverse scans across ε-Ga_2O_3 (0004) (solid black line) and (10$\bar{1}$4) (dashed-dotted blue line) reflections with full-width at half maxima (FWHM). (b) (c) Side-view schematics of ε-Ga_2O_3 (0001) and In_2O_3 (111) planes, respectively. Dashed-dotted lines indicate bulk-terminated surfaces. Ga, In and O atoms are depicted in gold, red and blue, respectively. (d) Top view of ε-Ga_2O_3 (0001) and In_2O_3 (111). Dashed lines illustrate 5:4 coincidence lattice of O-terminated ε-Ga_2O_3 (0001) relative to indium-terminated In_2O_3 (111).

The researchers used PAMBE on the (0001) surface of α-aluminium oxide (sapphire) substrates. The growth started with 20nm β-Ga_2O_3 nucleation. In further growth, the team found that the presence of indium catalyzes the growth of Ga_2O_3 in 700ºC conditions where no growth occurs in the absence of indium (Figure 7). At the same time, the indium is not incorporated into the growing Ga_2O_3 crystal structure. "This effect should not be confused with that of a surfactant, which either inhibits or induces a morphological phase transition but does not affect the growth rate of the material," the researchers warn.

The team explains the effect in terms of two steps: first, the formation of In_2O_3 is kinetically favored over Ga_2O_3 by a factor of 2.8; second, however, In_2O_3 is unstable in the presence of Ga, and energy factors favor indium replacement by gallium.

X-ray analysis suggested that the Ga_2O_3 grown with indium catalysis does not correspond to the underlying nucleation layer with the reflections shifted to larger angles. The team reports; "The angular position of these reflections perfectly agrees with those of the 0002 and 0004 reflections of the metastable ε-Ga_2O_3 phase, which crystallizes in a hexagonal structure ($P6_3mc$)."

Further x-ray and electron diffraction analysis confirmed the ε-Ga_2O_3 attribution, according to the researchers. "Clearly, the profiles reveal a well-oriented epitaxial film, which is particularly remarkable since films in the ε phase could not yet be obtained by PAMBE," they add.

The researchers see the ε-Ga_2O_3 (0001) structure as being better suited to heterostructures involving In_2O_3 (111) since the planes match in terms of symmetry, atomic spacing and surface chemistry (Figure 8). The researchers comment: "the two lattices are in almost perfect registry when forming a 5:4 coincidence lattice with a residual mismatch of 1.3%."

The researchers suggest that the metal-catalysis could apply to systems with similar kinetic and thermodynamic properties: "For example, we recently showed that the oxidation efficiency of Sn (η_{Sn}) is even larger than that of indium, which, in turn, is larger than that of gallium, i.e. $\eta_{Sn} > \eta_{In} > \eta_{Ga}$. Thus, we expect catalytic effects for a wide range of ternary oxide alloys, but also for various other multi-component oxides fabricated by MBE." ■

The researchers hope that their work will be a path for bandgap engineering and heterostructural growth of transparent semiconducting oxides. They see analogies with the III–V world, where heterostructures of semiconductor alloys have created a vast range of optoelectronic and telecom devices. For the sesquioxides, the team suggests applications in deep-ultraviolet detection, transparent transistors, and high-power electronics

Author: Mike Cooke is a freelance technology journalist who has worked in the semiconductor and advanced technology sectors since 1997.